Photocatalytic Activity for Water Decomposition of Indates with Octahedrally Coordinated d^{10} Configuration. I. Influences of Preparation Conditions on Activity

J. Sato, N. Saito, H. Nishiyama, and Y. Inoue*

Department of Chemistry, Nagaoka University of Technology, Nagaoka 940-2188, Japan

Received: January 9, 2003; In Final Form: April 23, 2003

The photocatalytic properties for water decomposition of RuO_2-dispersed alkaline earth metal and lanthanum indates with an octahedrally coordinated In^{3+} ion of d^{10} configuration were studied. The influences of preparation methods, calcination temperature, and the amount of RuO_2 on the activity of RuO_2-dispersed $CaIn_2O_4$ were examined, and it was shown that the combination of well-crystallized $CaIn_2O_4$ with highly dispersed RuO_2 particles led to high photocatalytic performance: hydrogen and oxygen were stably produced at nearly the stoichiometric ratio under UV irradiation. The photocatalytic activity of RuO_2-dispersed $Sr_{1-x}Ca_xIn_2O_4$ (x = 0.25, 0.50, 0.75) increased monotonically with increasing x. The activity of RuO_2-dispersed $Sr_{0.93}Ba_{0.07}In_2O_4$ was similar to that of RuO_2-dispersed $SrIn_2O_4$, whereas RuO_2-dispersed $LaInO_3$ had much lower activity. The photocatalytic properties of different kinds of indates were compared.

Introduction

In previous studies, we have demonstrated that the p-block metal oxides of MIn_2O_4,[1,2] M_2SnO_4,[1] $M_2Sb_2O_7$ (M = Ca, Sr),[3] $CaSb_2O_6$,[3] $NaSbO_3$,[3] and $ZnGa_2O_4$[4] make good photocatalysts for water decomposition by the dispersion of RuO_2 particles on these metal oxides. The electronic structures of the p-block metal oxides are composed of octahedrally coordinated metal ions with d^{10} configuration. This is an interesting characteristic feature, since almost all of the photocatalysts developed in the past two decades for water decomposition have consisted of transition metal oxides involving octahedrally coordinated d^0 metal ions of Ti^{4+}, Zr^{4+}, Nb^{5+}, and Ta^{5+}, which have mostly been used in combination with NiO and RuO_2 as a promoter.[5−21]

For further development of RuO_2-combined p-block d^{10} metal oxides for water decomposition, it is of importance to reveal their photocatalytic properties and to shed light on the electronic and geometric structures that control the characteristic photocatalysis. In a previous communication, we have briefly reported that RuO_2-dispersed MIn_2O_4 (M = Ca, Sr) have stable and large photocatalytic activities for water decomposition.[1,2] Thus, various kinds of the indates with octahedrally coordinated In^{3+} are considered to be an interesting target. In the present work, alkaline earth metal indates of $CaIn_2O_4$, $SrIn_2O_4$, $Sr_{1-x}Ca_xIn_2O_4$ (x = 0.25, 0.50, 0.75), $Sr_{1-x}Ba_xIn_2O_4$ (x = 0.07), and lanthanum indate of $LnInO_3$ (Ln = La, Nd) were chosen. The photocatalytic performance was compared among the different kinds of indates. The influences of preparation methods, calcination temperature, and the amount of dispersed RuO_2 on the photocatalytic activities were investigated in detail for $CaIn_2O_4$, and the photocatalytic conditions for the achievement of high activity are discussed.

Experimental Section

Calcium indate, $CaIn_2O_4$, was synthesized by two methods. First, $Ca(NO_3)_2{\cdot}4H_2O$ (Wako, 99.9% pure) and $In(NO_3)_3{\cdot}3H_2O$ (Nacalai Tesque, EP grade) were dissolved in a water−ethanol mixture, and an oxalic acid−ethanol solution was added. The coprecipitate was aged at 353 K, dried at 393 K, and calcined at different temperatures from 1273 to 1573 K. Second, calcium and indium carbonate were mechanically mixed in an equimolar ratio in an agate and calcined in air at high temperatures. To distinguish the prepared calcium indates, the notation of (m) was attached, such as $CaIn_2O_4$(m) for preparation by the second method. For $SrIn_2O_4$ and $Sr_{1-x}Ba_xIn_2O_4$, the coprecipitates were prepared under similar conditions with $Sr(NO_3)_2$ (Nacalai Tesque, ER grade) and $Ba(NO_3)_2$ (Junsei Chemical Co., 99% pure) and were calcined in air at 1373 K for 16 h. $LaInO_3$ was prepared by calcination of a molar mixture of La_2O_3 (Nacalai Tesque, GR grade) and In_2O_3 in air in the temperature range 1373−1573 K for 16 h. The formation of the prepared indates was confirmed by X-ray diffraction patterns obtained with a Rigaku RAD III diffractometer.

The loading of RuO_2 on the metal oxides was performed by an impregnation method in a similar manner as described elsewhere.[1−4] Briefly, the prepared indates were impregnated with ruthenium complex, $Ru_3(CO)_{12}$ (Aldrich Chemical Co., 99% pure) in tetrahydrofuran (THF), dried at 333 K, and oxidized at 673 K in air to convert ruthenium complex species to ruthenium oxide.

The photocatalytic reaction was performed in a closed gas-circulating apparatus equipped with a quartz reaction cell. About 250 mg of photocatalyst was placed in ion-exchanged and distilled water in the quartz reaction cell. The reaction system was filled with 1.33 kPa of Ar gas that was circulated with a glass piston pump during the photocatalytic reaction. Powder photocatalysts were dispersed in the water by stirring of Ar gas bubbling and were irradiated with a 400 W Xe lamp with a wavelength of 280−700 nm (Ushio VI-501C) or a 200 W Hg−Xe lamp with a wavelength of 230−436 nm (Hamamatsu L5662). H_2 and O_2 produced in the gas phase were analyzed by an on-line gas chromatograph.

Surface area was measured on a Yuasa Chembet-3000 apparatus by a Brunauer−Emmett−Teller (BET) method. UV diffuse reflectance spectra were recorded on a Jasco Uvidec-660. Scanning electron microscopic (SEM) images were obtained by a JEOL-JXA733 spectroscope at a magnification of 2000−10 000.

10.1021/jp030020y CCC: $25.00
Published on Web 07/12/2003

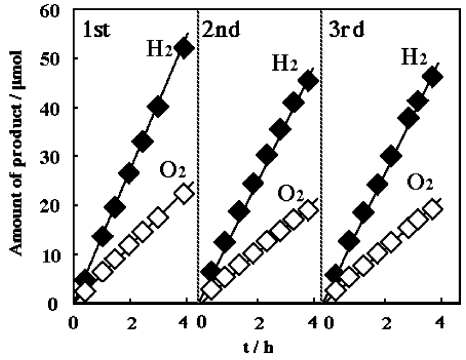

Figure 1. Repeated run of water decomposition on 1 wt % RuO_2-dispersed $CaIn_2O_4$. $CaIn_2O_4$ was prepared by calcination at 1373 K.

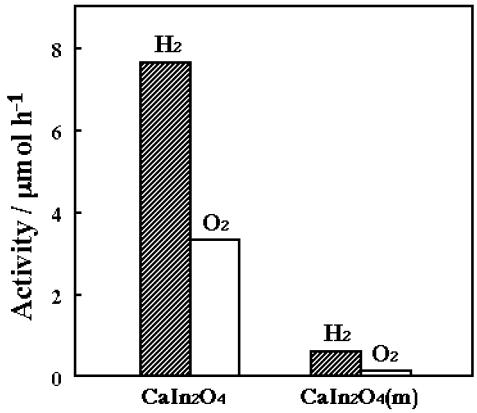

Figure 2. Comparison of activity of 1 wt % RuO_2-dispersed $CaIn_2O_4$ and $CaIn_2O_4$(m). Both $CaIn_2O_4$ and $CaIn_2O_4$(m) were calcined at 1273 K.

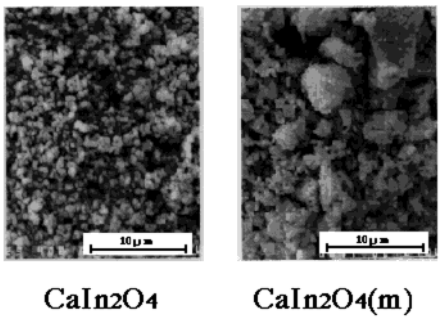

Figure 3. Scanning electron microscope images of $CaIn_2O_4$ and $CaIn_2O_4$(m) calcined at 1273 K.

Results

Figure 1 shows photocatalytic water decomposition on 1 wt % RuO_2-dispersed $CaIn_2O_4$ under Xe lamp illumination. The reaction was repeated three times. From the initial stage of irradiation in the first run, both hydrogen and oxygen were produced in a H_2/O_2 ratio of 2.2, and their amounts increased in proportion to irradiation time. The photocatalytic activity slightly decreased in the second run, but no further attenuation occurred in the third run, indicating that RuO_2-dispersed $CaIn_2O_4$ photocatalysts were stable.

Figure 2 compares the photocatalytic activity of 1 wt % RuO_2-dispersed $CaIn_2O_4$ and $CaIn_2O_4$(m). The former provided approximately 13-fold higher photocatalytic activity and a better H_2/O_2 ratio than did the latter. Figure 3 shows the SEM images of $CaIn_2O_4$ and $CaIn_2O_4$(m). Very fine particles were observed for $CaIn_2O_4$, whereas for $CaIn_2O_4$(m) the particle size was not uniform and large particles were present.

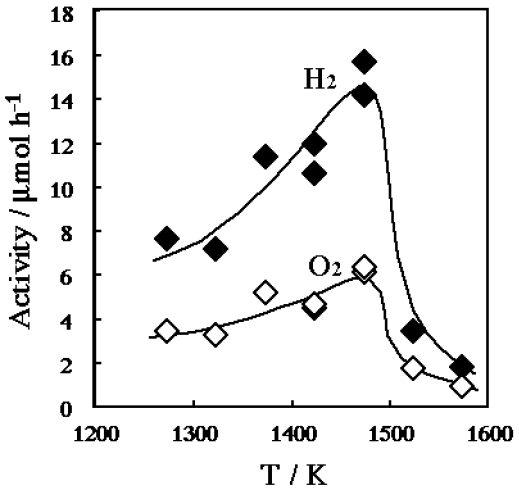

Figure 4. Changes in photocatalytic activity of 1 wt % RuO_2-dispersed $CaIn_2O_4$ with calcination temperature of $CaIn_2O_4$.

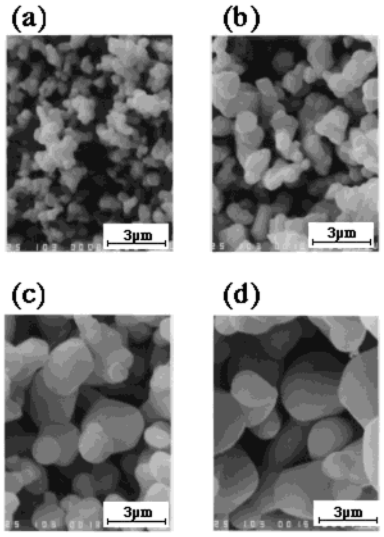

Figure 5. Scanning electron microscopic images of $CaIn_2O_4$ treated by calcination at 1373 (a), 1473 (b), 1523 (c), and 1573 K (d).

Figure 4 shows the photocatalytic activity of 1 wt % RuO_2-dispersed $CaIn_2O_4$ as a function of calcination temperature of $CaIn_2O_4$. With increasing calcination temperatures, the photocatalytic activity increased considerably from 1273 K, passed through a maximum at around 1473 K, and decreased sharply above 1500 K. In the X-ray diffraction patterns for $CaIn_2O_4$ calcined at 1273 K, major peaks appeared at $2\theta = 32.0°$, 33.4°, and 47.1°, which were assigned to the diffractions from the (320), (121), and (401) planes, respectively. The diffraction pattern was consistent with that reported previously[22] and remained unchanged up to 1573 K. With increasing calcination temperatures, however, the width of the major diffraction peaks became narrower. The surface area of $CaIn_2O_4$ was 3.3 $m^2\ g^{-1}$ for 1273 K, decreased to 1.8 $m^2\ g^{-1}$ for 1373 K, to 0.8 $m^2\ g^{-1}$ for 1473 K, and to 0.3 $m^2\ g^{-1}$ for 1573 K-calcined $CaIn_2O_4$. The surface area of $CaIn_2O_4$(m) calcined at 1273 K was smaller by a factor of 1.9 than that of $CaIn_2O_4$ treated at the same temperature.

Figure 5 shows the SEM images of $CaIn_2O_4$ calcined at different temperatures. The particles of $CaIn_2O_4$ subjected to calcination at 1273 K were small and irregular rugged shapes, as shown in Figure 3. The particles grew by calcination from 1323 to 1473 K, losing the rugged feature. The particle shape changed to be spherical at around 1473 K, which was indicative

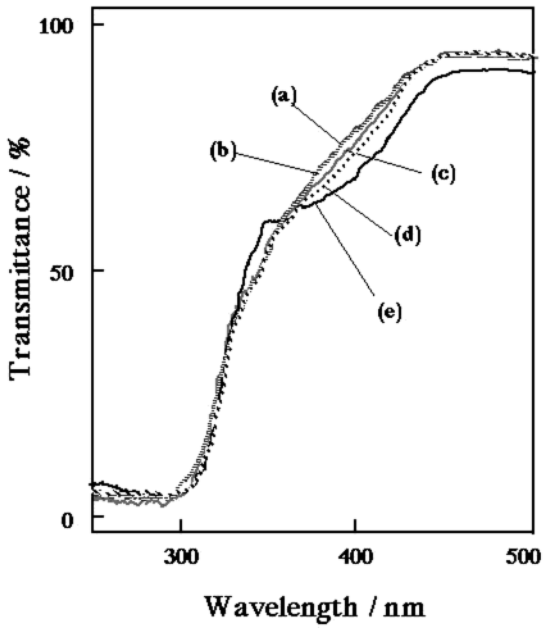

Figure 6. UV diffuse reflectance spectra of $CaIn_2O_4$ treated by calcination at 1273 (a), 1373 (b), 1473 (c), 1523 (d), and 1573 K (e).

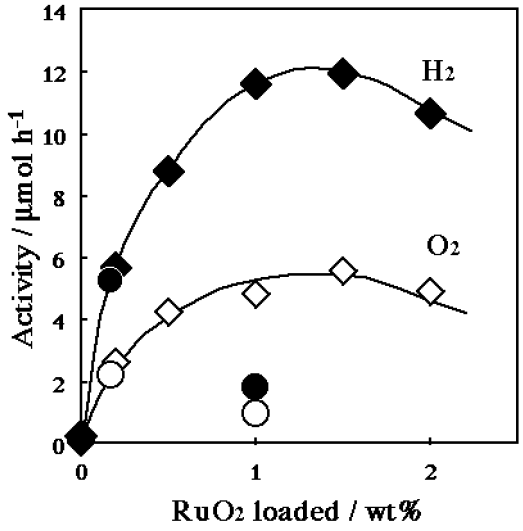

Figure 7. Photocatalytic activity of RuO_2-dispersed $CaIn_2O_4$ as a function of RuO_2 amount: H_2 (◆) and O_2 (◇) for $CaIn_2O_4$ calcined at 1423 K; H_2 (●) and O_2 (○) for $CaIn_2O_4$ calcined at 1573 K.

of the agglomeration of particles. The particles grew markedly in the temperature range 1523−1573 K. These results, together with narrower diffraction peaks, indicated that crystallization proceeded by calcination from 1323 to 1473 K, followed by marked sintering in the temperature range 1523−1573 K.

Figure 6 shows the UV diffuse reflectance spectra of $CaIn_2O_4$ calcined in the temperature range 1273−1573 K. $CaIn_2O_4$ calcined at 1273 K showed the threshold absorption at around 450 nm and gradual and slightly steep absorption between 420 and 310 nm. The absorption reached a maximum at 305 nm. Nearly the same absorption characteristics were observed when $CaIn_2O_4$ was calcined in the temperature range 1373−1473 K, but a broad bump appeared at around 400 nm for 1423 K-calcined $CaIn_2O_4$ and grew with increasing calcination temperatures.

Figure 7 shows changes in the photocatalytic activity with the amount of RuO_2 dispersed on 1423 K-calcined $CaIn_2O_4$. In the absence of RuO_2, only a small amount of hydrogen was produced, and the photocatalytic activity was negligible. The

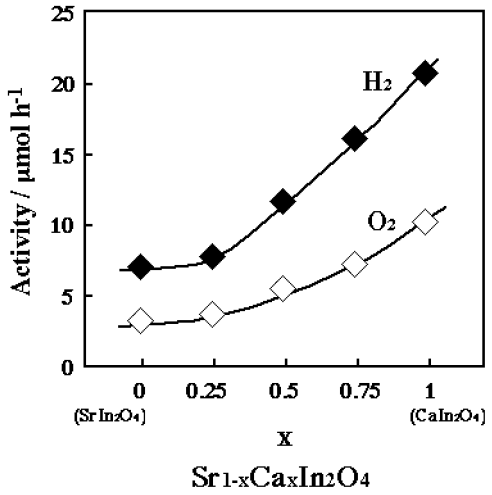

Figure 8. Photocatalytic activity of 1 wt % RuO_2-dispersed $Sr_{1-x}Ca_xIn_2O_4$ as a function of x. $Sr_{1-x}Ca_xIn_2O_4$ was calcined at 1373 K.

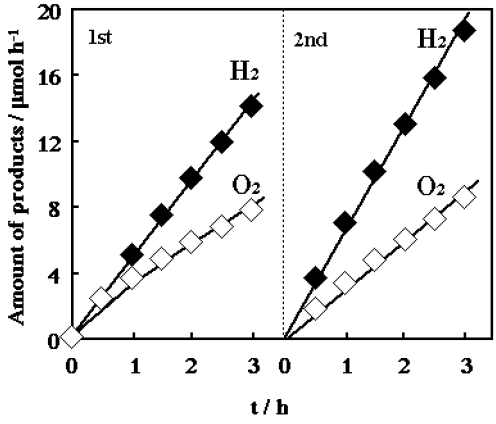

Figure 9. H_2 and O_2 production from water on 1 wt % RuO_2-dispersed $Sr_{0.93}Ba_{0.07}In_2O_4$. $Sr_{0.93}Ba_{0.07}In_2O_4$ was calcined at 1373 K.

addition of 0.25 wt % RuO_2 led to remarkable photocatalytic activity for both H_2 and O_2 productions. The activity increased significantly in 0.25−1.0 wt % RuO_2 and reached a plateau at around 1−1.5 wt %. Further increase to 2 wt % caused a slight activity fall. Figure 7 also shows the effects of the amount of RuO_2 dispersed on 1573 K-calcined $CaIn_2O_4$. Irrespective of a decrease in RuO_2 amount from 1.0 to 0.17 wt %, the activity augmented by a factor of 2.9. It should be noted that the activity enhancement for 1573 K-calcined $CaIn_2O_4$ with decreasing amount of RuO_2 is opposite to the activity fall observed for 1423 K-calcined $CaIn_2O_4$ in a similar regime of RuO_2 amount.

Figure 8 shows the photocatalytic activity of RuO_2-dispersed $Sr_{1-x}Ca_x$ In_2O_4 as a function of x. The activity monotonically increased with increasing x. In the UV diffuse reflectance spectra of $Sr_{1-x}Ca_xIn_2O_4$, the absorption started at around 450 nm and reached the highest level at 300 nm irrespective of x.

Figure 9 shows water decomposition on RuO_2-dispersed $Sr_{0.93}$-$Ba_{0.07}In_2O_4$. The productions of hydrogen and oxygen were observed in repeated runs, and the ratio of H_2/O_2 was 2.2. The UV diffuse reflectance spectrum showed that light absorption characteristics of $Sr_{0.93}Ba_{0.07}In_2O_4$ were nearly the same as those observed for MIn_2O_4 (M = Ca, Sr).

Figure 10 shows the productions of hydrogen and oxygen on RuO_2-dispersed $LaInO_3$ under Hg−Xe lamp irradiation. In three runs, nearly the same production levels were observed, indicative of the stability of the photocatalysts. The dependence of activity on calcination temperature was compared at 1373,

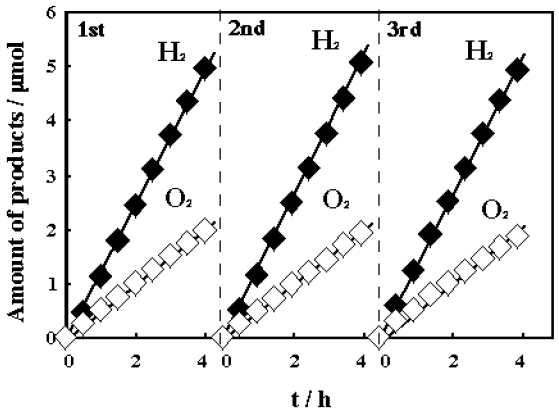

Figure 10. H_2 and O_2 production from water on 1 wt % RuO_2-dispersed $LaInO_3$ under Hg−Xe lamp irradiaiton. $LaInO_3$ was calcined at 1473 K.

1473, and 1573 K. The activity of $LaInO_3$ calcined at 1473 K was higher by a factor of 2.5 and 3.4 compared to that calcined at 1373 and 1573 K, respectively. The ratio of H_2/O_2 was 2.8. The UV diffuse reflectance spectrum showed a threshold absorption wavelength at 480 nm, main absorption in the wavelength region 450−350 nm, and the highest level at 280 nm. However, it should be noted that a little activity was observed under the conditions of Xe lamp irradiation instead of Hg−Xe lamp irradiation. The activity of RuO_2-loaded $NdInO_3$ with Nd instead of La was examined under Hg−Xe lamp irradiation, but neither hydrogen nor oxygen was produced to a detectable level. The order of photocatalytic activity obtained under Xe lamp illumination was $CaIn_2O_4 > SrIn_2O_4$, $Sr_{0.93}Ba_{0.07}In_2O_4 \gg LaInO_3$, $NdInO_3$.

Discussion

The combination of MIn_2O_4 (M = Ca, Sr) with RuO_2 produced H_2 and O_2 in nearly stoichiometric ratio under Xe lamp irradiation, and the production was reproducible in repeated runs. In comparison of the preparation methods, the photocatalytic activity of $CaIn_2O_4$ prepared from the coprecipitates was 13 times larger than that prepared from a mechanical mixture of the starting materials. The SEM observation demonstrated that the higher activity was due to the formation of fine $CaIn_2O_4$ particles by coprecipitation. The activity of RuO_2-dispersed $CaIn_2O_4$ was strongly dependent on the calcination temperature of $CaIn_2O_4$: it increased remarkably between 1273 and 1473 K. In the same temperature range, as shown in the SEM images, the size of $CaIn_2O_4$ particles increased considerably, and the X-ray diffraction peak became narrower. These results indicate that the crystallization of $CaIn_2O_4$ proceeds markedly over the temperature range. Thus, the activity rise with increasing temperatures up to 1473 K is due to the elimination, through crystallization, of impurities and structural imperfections that work as recombination sites for photoexcited charges. The photocatalytic activity reached a maximum level at around 1473 K, above which a dramatic decrease occurred. In the high calcination temperature region, the extraordinary growth of $CaIn_2O_4$ particles was observed, accompanied by a sharp drop of surface area. Thus, it is evident that the activity decrease is related to significant decreases in the surface area of $CaIn_2O_4$. The photon efficiency of RuO_2-dispersed $CaIn_2O_4$ with the highest activity was very roughly estimated to be 5% from a comparison of the photocatalytic activity with previous results.[8]

In the correlation between the amount of dispersed RuO_2 and photocatalytic activity (Figure 7), the activity decreased in a higher RuO_2 concentration regime. Furthermore, as shown in Figure 7, in the case where the amount of RuO_2 loaded was intentionally reduced from 1.0 to 0.17 wt % for $CaIn_2O_4$ with a small surface area, the activity increased approximately 3-fold. It is apparent that the excess amount of RuO_2 leads to low photocatalytic activity. The agglomeration of RuO_2 particles readily occurs when large amounts of RuO_2 were loaded for a small surface area of $CaIn_2O_4$, producing large RuO_2 particles, which results in decreases of the density of photocatalytic active sites. These results indicate that a high dispersion of small RuO_2 particles is essential for high photocatalytic performance of RuO_2-dispersed $CaIn_2O_4$. The previous X-ray photoelectron spectroscopy showed that the binding energy of $Ru3d_{5/2}$ level for the Ru complex dispersed on $ZnGa_2O_4$ was 280.7 eV when oxidized at 573 K.[4] The binding energy was the same, within measurement accuracy, as that for RuO_2 powder and Ru powder oxidized at 823 K. The same oxidation temperature was employed here, and it is likely that the Ru species exists as Ru^{4+}, forming $Ru(IV)O_2$ particles as an active promoter.

The photocatalytic activity of RuO_2-dispersed $CaIn_2O_4$ was 3 times larger than that of RuO_2-dispersed $SrIn_2O_4$. The activity of RuO_2-dispersed $Sr_{1-x}Ca_xIn_2O_4$ increased monotonically with increasing x. $CaIn_2O_4$ has an orthorhombic structure with a unit cell of $a = 0.965$, $b = 1.13$, and $c = 0.321$ nm,[23] and $SrIn_2O_4$ has the same orthorhombic structure with lattice parameters of $a = 0.9809$, $b = 1.1449$, and $c = 0.3265$ nm.[24] $CaIn_2O_4$ and $SrIn_2O_4$ have nearly the same crystal structure, but the size of the unit cell is slightly smaller for $CaIn_2O_4$. It is reasonable to consider that a continuous change in the unit cell with x is responsible for the monotonic activity enhancement. $Sr_{0.93}Ba_{0.07}In_2O_4$ has a similar orthorhombic crystal structure with lattice parameters of $a = 0.9858$, $b = 1.152$, and $c = 0.3273$ nm.[25] The similarity of activity to that of $SrIn_2O_4$ results from little difference in the crystal structures.

The photocatalytic activity for water decomposition under Xe lamp illumination was considerably large for RuO_2-dipsersed $CaIn_2O_4$, $SrIn_2O_4$, and $Sr_{0.93}Ba_{0.07}In_2O_4$ but was very poor for RuO_2-dispersed $LnInO_3$ (Ln = La, Nd). A study also showed that the photocatalytic activity of RuO_2-dispersed $AInO_2$ (A = Li, Na) was negligible under Xe lamp illumination.[26] These results exhibited that alkaline earth metal indates possessed high ability to photocatalytically decompose water and also that there were clear differences in the photocatalytic properties among the indates, even though they all were composed of an octahedrally coordinated In^{3+} (d^{10}) metal ion. It is strongly desirable to elucidate the activity differences, which will be discussed in detail on the basis of the geometric and electronic structures of indates in the companion paper.[26]

Acknowledgment. This work was supported by CREST of JSP and a Grant-in-Aid of the Priority area of research scientific fund (15033229) from The Ministry of Education, Science, Sports and Culture.

References and Notes

(1) Sato, J.; Saito, S.; Nishiyama, H.; Inoue, Y. *J. Phys. Chem.* **2001**, *105*, 6061.

(2) Sato, J.; Saito, S.; Nishiyama, H.; Inoue, Y. *Chem. Lett.* **2001**, 868.

(3) Sato, J.; Saito, S.; Nishiyama, H.; Inoue, Y. *J. Photochem. Photobiol. A: Chem.* **2002**, *148*, 85.

(4) Ikarashi, K.; Sato, J.; Kobayashi, H.; Saito, S.; Nishiyama, H.; Inoue, Y. *J. Phys. Chem.* **2002**, *106*, 9048.

(5) Domen, K.; Kudo, A.; Onishi, T. *J. Catal.* **1986**, *102*, 92.

(6) Inoue, Y.; Kubokawa, T.; Sato, K. *J. Phys. Chem.* **1991**, *95*, 4059.

(7) Ogura, S.; Kohno, M.; Sato, K.; Inoue, Y. *Appl. Surf. Sci.* **1997**, *121/123*, 521.

(8) Inoue, Y.; Asai, Y.; Sato, K. *J. Chem. Soc., Faraday Trans.* **1994**, *90*, 797.
(9) Kohno, M.; Kaneko, T.; Ogura, S.; Sato, K.; Inoue, Y. *J. Chem. Soc., Faraday Trans.* **1998**, *94*, 89.
(10) Takata, T.; Furumi, Y.; Shinohara, K.; Tanaka, A.; Hara, M.; Kondo, J. N.; Domen, K. *Chem. Mater*. **1997**, *9*, 1063.
(11) Takata, T.; Shinohara, K.; Tanaka, A.; Hara, M.; Kondo, J. N.; Domen, K. *J. Photochem. Photobiol. A: Chem*. **1997**, *106*, 45.
(12) Sayama, K.; Arakawa, H. *J. Phys. Chem*. **1993**, *97*, 531.
(13) Kudo, A.; Tanaka, A.; Domen, K.; Maruya, K.; Aika, K.; Onishi, T. *J. Catal*. **1998**, *111*, 67.
(14) Kudo, A.; Kato, H.; Nakagawa, S. *J. Phys. Chem. B.* **2000**, *104*, 571.
(15) Kato, H.; Kudo, A. *Catal. Lett*. **1999**, *58*, 153.
(16) Ishihara, T.; Nishiguchi, H.; Fukamachi, K.; Takita, Y. *J. Phys. Chem. B* **1999**, *103*, 1.
(17) Kato, H.; Kudo, A. *Chem. Phys. Lett*. **1998**, *295*, 487.
(18) Kato, H.; Kudo, A. *Chem. Lett*. **1999**, 1027.
(19) Ogura, S.; Kohno, M.; Sato, K.; Inoue, Y. *Phys. Chem. Chem. Phys.* **1999**, *1*, 179.
(20) Kohno, M.; Ogura, S.; Sato, K.; Inoue, Y. *J. Chem. Soc., Faraday Trans.* **1997**, *93*, 2433.
(21) Kohno, M.; Ogura, S.; Sato, K.; Inoue, Y. *Chem. Phys. Lett*. **1997**, *267*, 72.
(22) JCPDS file, 17-0643.
(23) Criuckshank, F. R.; Taylor, D. MaK.; Glasser, F. P. *J. Inorg. Nucl. Chem*. **1964**, *26*, 937.
(24) Von Schenck, R.; Mueller-Buschbaum, H. *Z. Anorg. Allg. Cehm*. **1973**, *398*, 24.
(25) Lalla, A.; Mueller-Buschbaum, H. *Z. Anorg. Allg. Cehm*. **1990**, *588*, 117.
(26) Sato, J.; Kobayashi, H.; Inoue, Y. *J. Phys. Chem B* **2003**, *107*, 7970 (following paper in this issue).